

WEAR-RESISTANT SINGLE-PHASE HIGH-ENTROPY ALLOY COATINGS PREPARED ON Ti6Al4V WITH LASER CLADDING

OBRABNO OBSTOJNA ENOFAZNA VISOKO-ENERGIJSKA PREVLEKA, NANEŠENA Z LASERSKIM NAVARJANJEM NA OSNOVO IZ ZLITINE Ti6Al4V

Yongfei Juan, Jun Li*, Yunqiang Jiang, Wanli Jia, Zhongjie Lu

Shanghai University of Engineering Science, School of Materials Engineering, No. 333 Longteng Road, Songjiang District, 201620 Shanghai, China

Prejem rokopisa – received: 2019-01-22; sprejem za objavo – accepted for publication: 2019-05-17

doi:10.17222/mit.2019.018

Excellent wear-resistant high-entropy alloy (HEA) coatings were successfully synthesized on Ti6Al4V with laser cladding using FeCrCoNiAlMo_x ($x = 0.5, 1.0, 1.5$) as the cladding materials. Investigations into the effect of Mo on the microstructures and mechanical properties (microhardness and wear resistance) of the coatings were carried out. The results showed that all the coatings exhibited good metallurgical bonding with the substrate where no clear defects were found. The dilution rate of the coatings increased with an increase in the content of Mo (60.39 % for $x = 0.5$, 64.09 % for $x = 1.0$, 72.68 % for $x = 1.5$). The coating for $x = 1.0$ was mainly composed of a single solid solution (BCC). Besides the solid solution, traces of TiC dendrites were also synthesized in the other two coatings ($x = 0.5$ and $x = 1.5$). The solid solution exhibited two different morphologies, corresponding to fine rod-like particles and coarse equiaxial grains. Due to the solution- and dispersion-strengthening effects, the hardness of the coatings (759.4 HV_{0.2} for $x = 0.5$, 857.2 HV_{0.2} for $x = 1.0$, 844.3 HV_{0.2} for $x = 1.5$) was significantly superior to that of the substrate (330 HV_{0.2}). The friction coefficient of the coatings (0.80 for $x = 0.5$, 0.61 for $x = 1.0$ and 0.78 for $x = 1.5$) was obviously reduced when compared with that of the substrate (1.04). The wear volumes of the coatings were decreased by 51 %, 65 % and 48 % ($1.145 \pm 0.021 \text{ mm}^3$ for $x = 0.5$, $0.823 \pm 0.012 \text{ mm}^3$ for $x = 1.0$, $1.219 \pm 0.018 \text{ mm}^3$ for $x = 1.5$) when compared with that of the substrate ($2.329 \pm 0.025 \text{ mm}^3$). It can be confirmed that the coating with $x = 1.0$ exhibited the optimum wear resistance.

Keywords: laser cladding, high-entropy alloy, Ti6Al4V, wear resistance

Avtorji so uspešno sintetizirali obrabno obstojno prevleko na osnovi visoko-entropijske zlitine (HEA; angl.: High Entropy Alloy) na podlago iz Ti6Al4V, z laserskim navarjanjem. Za navarjanje so uporabili zlitino na osnovi FeCrCoNiAlMo_x ($x = 0.5, 1.0, 1.5$). Izvedli so tudi raziskave vpliva Mo na mikrostrukture in na mehanske lastnosti (mikrotrdoto in odpornost proti obrabi) prevleke. Rezultati so pokazali, da imajo prevleke dobro metalurško povezavo s podlago, na kateri sicer niso našli jasnih napak. Hitrost raztapljanja prevleke s podlago je naraščala s povečevanjem vsebnosti Mo (60,39 % za $x = 0.5$, 64,09 % za $x = 1,0$ in 72,68 % za $x = 1,5$). Prevleka z $x = 1,0$ je bila v glavnem enofazna homogena trdna raztopina s telesno centrirano kubično zgradbo (BCC; angl.: Body Cubic Centred). Poleg homogene trdne raztopine so se v drugih dveh sintetiziranih prevlekah, $x = 0,5$ in $x = 1,5$, nahajali še sledovi dendritov TiC. Trdna raztopina je imela dve različni morfologiji s finimi paličastimi delci in grobimi enakoosnimi kristalnimi zrni. Zaradi učinkov raztapljanja in disperzije so imele prevleke v primerjavi s podlago (330 HV_{0.2}) precej višje trdote: 759,4 HV_{0.2} za $x = 0,5$, 857,2 HV_{0.2} za $x = 1,0$, 844,3 HV_{0.2} za $x = 1,5$. Koeficient trenja prevlek: 0,80 za $x = 0,5$, 0,61 za $x = 1,0$ in 0,78 za $x = 1,5$, se je očitno zmanjšal v primerjavi s podlago (1,04). Volumska obraba je bila manjša za 51%, 65% in 48% ($1,145 \pm 0,021 \text{ mm}^3$ za $x = 0,5$, $0,823 \pm 0,012 \text{ mm}^3$ za $x = 1,0$ in $1,219 \pm 0,018 \text{ mm}^3$ za $x = 1,5$) v primerjavi s podlago ($2,329 \pm 0,025 \text{ mm}^3$). Avtorji zaključujejo, da je imela prevleka s sestavo $x = 1,0$ optimalno odpornost proti obrabi.

Ključne besede: lasersko navarjanje, visoko-energijska zlitina, Ti6Al4V, odpornost proti obrabi

1 INTRODUCTION

In modern industry, benefited from the excellent properties such as low density, high strength, excellent corrosion resistance and biocompatibility,¹ titanium alloys have been applied to various fields, such as aerospace, marine industries, petrochemical and medical application. However, poor wear resistance and low hardness seriously restrict their wider application.² At present, nitriding is the main method for improving the wear resistance of titanium alloys. Yang et al. applied intermittent vacuum gas nitriding (IVGN) to improve the wear resistance of the TB8 titanium alloy.³ A dense

nitride layer and a nitrogen diffusion zone formed on the alloy surface after heat treatment at 780 °C for 4 h. The hardness of the sample reached 850–900 HV. The friction coefficient of the nitrided sample (0.064–0.082 within 12 min) was clearly lower than that of the untreated sample (0.483), indicating that the wear resistance was greatly improved due to the formation of a gradient hardened layer.

S. Takesuea et al. developed a rapid nitriding process for titanium alloys at a low temperature, described as gas blow induction heating (GBIH) nitriding accompanied with fine-particle peening (FPP).⁴ Results showed that the nitrogen diffusion into titanium was accelerated by the pre-treatment with FPP during the GBIH nitriding process. Due to the formation of a hard nitrogen compound

*Corresponding author's e-mail:
jacob_ljun@sina.com

layer on the alloy surface, its wear resistance increased by about three times compared with that of the substrate, and its hardness (5.8 ± 1.3 GPa) was higher than that of the substrate (3.4 ± 0.3 GPa). In addition, other surface-engineering techniques such as physical vapor deposition (PVD) and micro-arc oxidation (MAO) are also adopted to enhance the wear resistance of titanium alloys. Unfortunately, the coatings synthesized with the above processes are usually thin ($0.1\text{--}5$ μm for PVD, $10\text{--}20$ μm for MAO, $20\text{--}30$ μm for nitriding),^{5–7} which greatly shortens their service life when a large impact load is applied to them in critical working conditions.

Comparatively speaking, laser cladding has attracted more attention in recent year. A good metallurgical bonding can be formed between the coatings and the substrates, the thickness of the coatings can reach up to the millimeter level, while their mechanical properties such as hardness and tensile strength can be flexibly adjusted by selecting different cladding materials.^{8–11} Many metal matrices reinforced with ceramic particles have been fabricated to improve the wear resistance of titanium alloys.¹² However, the presence of a large number of intermetallic compounds in laser-clad coatings can cause a decrease in plasticity, which reduces their machinability and increases their cracking susceptibility.

In recent twenty years, a new alloy-design concept of a high-entropy alloy (HEA) has attracted considerable attention. The main phase of such an alloy is a solid solution without or with traces of hard and brittle intermetallic compounds.¹³ The two shortcomings mentioned above can be overcome without significantly weakening the wear resistance. N. Tüten et al.¹⁴ prepared a TiTaHfNbZr HEA coating on Ti6Al4V using laser cladding. The average values of the Vickers hardness and elastic modulus of the HEA coating (12.51 ± 0.34 GPa and 181.3 ± 2.4 GPa) were higher than those of the substrate (3.46 ± 0.17 GPa and 115 ± 1.4 GPa). The friction coefficient of the coating (about 0.2) was about one third of that of the substrate (about 0.6), which indicated that the wear resistance of the coating was better than that of the substrate. H. Li et al.¹⁵ synthesized $\text{AlB}_x\text{CoCrNiTi}$ HEA coatings on Ti6Al4V using laser cladding. The coatings were mainly composed of the BCC phase. And due to the addition of B, the grain size of the coatings was refined. When x was 1.0, the hardness of the coating reached the highest value (814 HV) and the wear rate ($\text{mm}^3\cdot\text{h}^{-1}$) was one seventh of that of the coating without the addition of B. Obviously, deposition of protective HEA coatings on their surfaces with laser cladding is a very practical way to improve the wear resistance of titanium alloys.

Present investigations into a laser-clad HEA coating mainly focus on the selection and optimization of constituent elements for the cladding material so that the coating can be endowed with an excellent wear resistance on the basis of the solid solution as the main synthesized phase.¹⁶ Many studies have confirmed that simi-

lar atomic radii of different elements are beneficial to the formation of the solid solution for HEAs. Cr, Co, Fe and Ni are often selected as the main elements of HEAs due to their similar atomic radii (0.1248 nm for Co, 0.1241 nm for Fe, 0.1246 nm for Ni).^{17–20} However, the solution-strengthening effect is weakened to a certain extent for a solid solution composed of elements with similar atomic radii. Therefore, some non-metallic elements (such as B) and metallic elements with a great difference in the radius are often added to improve the solution-strengthening effect.²¹ The non-metallic elements easily react with the metallic elements, resulting in the formation of intermetallic compounds.²² When compared with the non-metallic elements, the metallic elements not only enhance the solution-strengthening effect, but also inhibit the formation of compounds.²³ Mo with excellent high-temperature strength and high hardness can be chosen as the other main strengthening element owing to its significant difference from Cr, Co, Fe, Ni in the atomic radius (0.1362 nm). However, excessive Mo in alloys may lead to the formation of unfavorable intermetallic compounds; therefore, it is extremely important to determine the appropriate Mo content in HEA coatings. Unfortunately, the effect of Mo on the microstructure and wear resistance of the laser-clad HEA coatings prepared on titanium alloys is hardly noted in present investigations.

Based on the above analyses, Cr, Co, Fe, Ni and Mo were chosen as the main constituent elements for the HEA coatings on Ti6Al4V applied with laser cladding in this work. Al was also added due to its positive effect in refining the grain size and improving the strength. The work comprehensively investigated the effect of Mo in FeCrCoNiAlMox ($x = 0.5, 1.0, 1.5$) on the microstructure, phase constituents, microhardness and wear resistance of the coatings. After that, the optimum amount of Mo was confirmed.

2 EXPERIMENTAL PART

The Ti6Al4V titanium alloy (annealed at 800 °C for one hour) was selected as the substrate and processed into a cylinder with a diameter of 50 mm and a height of 10 mm, then polished with 150-grit SiC abrasive papers and cleaned ultrasonically in acetone for 15 min before laser cladding. Pure Fe, Cr, Co, Ni, Al and Mo commercial powders were weighed in the three molar ratios (FeCrCoNiAlMox , $x = 0.5, 1.0, 1.5$) and mixed for 8 h in a ball grinding mill. A modified pre-placed method was applied to prepare the layer (**Figure 1**).²⁴ The substrate was placed into a hollow cylinder with a height of 11.0 mm and an inner diameter of 50.2 mm to allow the empty space with a height of 1.0 mm above the substrate. The organic binder (4 % polyvinyl alcohol) was pasted onto the substrate surface and then the empty space was filled with the mixed powder. Finally, the mixed powder was pressured by a tablet machine at 30 MPa with a

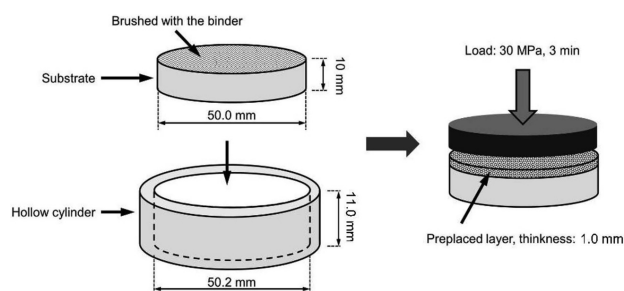


Figure 1: Schematic drawing of the preparation of the pre-placed layer

holding time of 3 min to form a pre-placed layer with a thickness of approximately 1.0 mm. An YLS-5000 fiber laser system was applied to obtain single-track coatings. The cladding parameters were as follows: a laser power of 3.0 kW, a spot diameter of 6 mm and a scanning speed of 5 mm/s.

The macromorphology and microstructure of the coatings were observed with a VHK-600 optical digital microscope and an S-3400 scanning electron microscope. A PANalytical X'Pert X-ray diffraction diffractometer and an EDAX energy dispersive spectrometer were used to analyze the phase constituents and chemical compositions of the coatings. The microhardness of the coatings was measured with an HXD-1000 TMSC/LCD Vicker's microhardness tester with a load of 1.96 N applied for 15 s. A CFT-1 ultra-functional wear-test machine was used to investigate the wear resistance of the coatings in dry-sliding conditions. Dry-sliding-wear test parameters were as follows: an applied load of 30 N, a reciprocating distance of 5 mm, a reciprocating sliding speed of $0.1 \text{ m}\cdot\text{s}^{-1}$, a wear test time of 180 min and the total distance of 1080 m. A 4-mm-diameter Si_3N_4 ball was chosen as the counterpart due to its excellent high-temperature stability (up to $1000 \text{ }^\circ\text{C}$) and high hardness (up to 35 GPa). The former makes Si_3N_4 retain its structural stability when exposed to a high temperature resulting from a lot of friction heat during dry-sliding. The latter can accelerate the wear of the test coatings in a short period. The contact stress between the friction pairs is closely related to the wear rate of the coatings. The initial contact stress can be calculated since the initial contact area is approximately constant. Based on the established contact model between the rigid sphere and the plane,²⁵ the initial Hertzian contact stress was calculated as 765 MPa.

3 RESULTS AND DISCUSSION

Figure 2 shows the cross-sectional macromorphologies of the coatings. The coatings are relatively smooth and no clear defects such as holes and cracks can be found. It can be observed that the thickness of the coatings increased with the increase in the content of Mo (2.64 mm for $x = 0.5$, 2.73 mm for $x = 1.0$ and 2.82 mm for $x = 1.5$). Further calculations show that the dilution

rate also presents the same change trend (60.39 % for $x = 0.5$, 64.09 % for $x = 1.0$, 72.68 % for $x = 1.5$), illustrating that an addition of the Mo element can significantly improve the bonding strength between the substrate and the coatings. This phenomenon is closely related to the high laser absorptivity of Mo. The laser absorptivity of Mo (0.43) is higher than those of the other elements (0.09 for Al, 0.26 for Ni, 0.33 for Co, 0.36 for Fe and 0.42 for Cr), meaning that more laser energy can be absorbed by the cladding material with a higher Mo content, causing a more serious melting of the substrate.

Figure 3 shows high-resolution micrographs of the interfaces in the coatings with different contents of Mo.

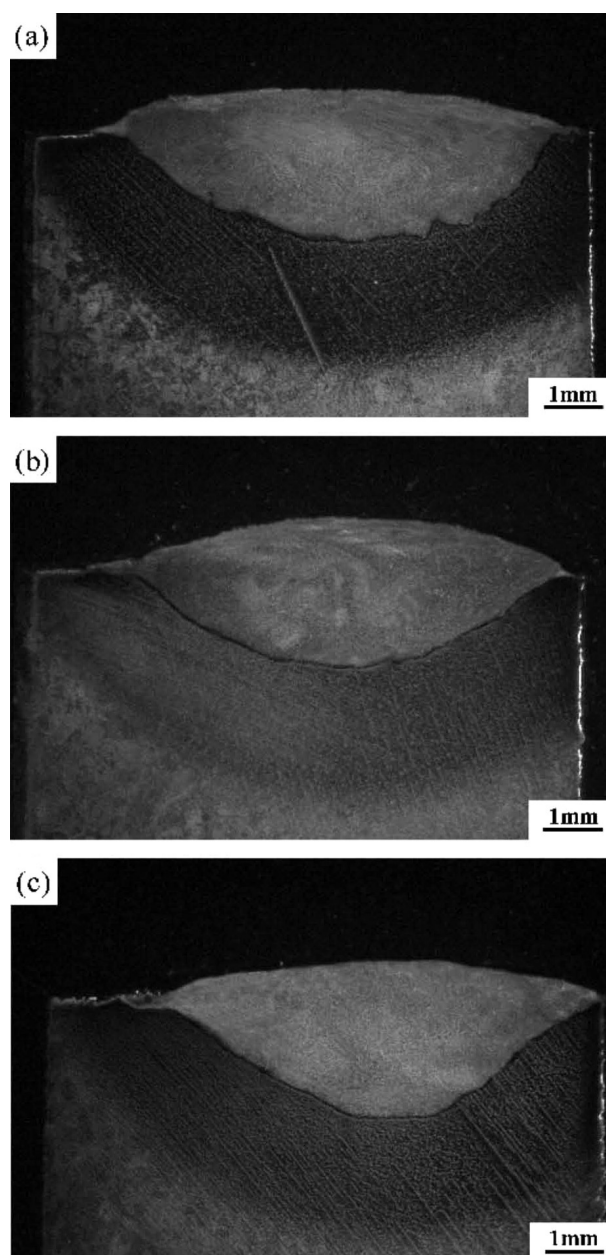


Figure 2: Macromorphology of the coatings with different contents of Mo: a) FeCrCoNiAlMo_{0.5}, b) FeCrCoNiAlMo_{1.0}, c) FeCrCoNiAlMo_{1.5}

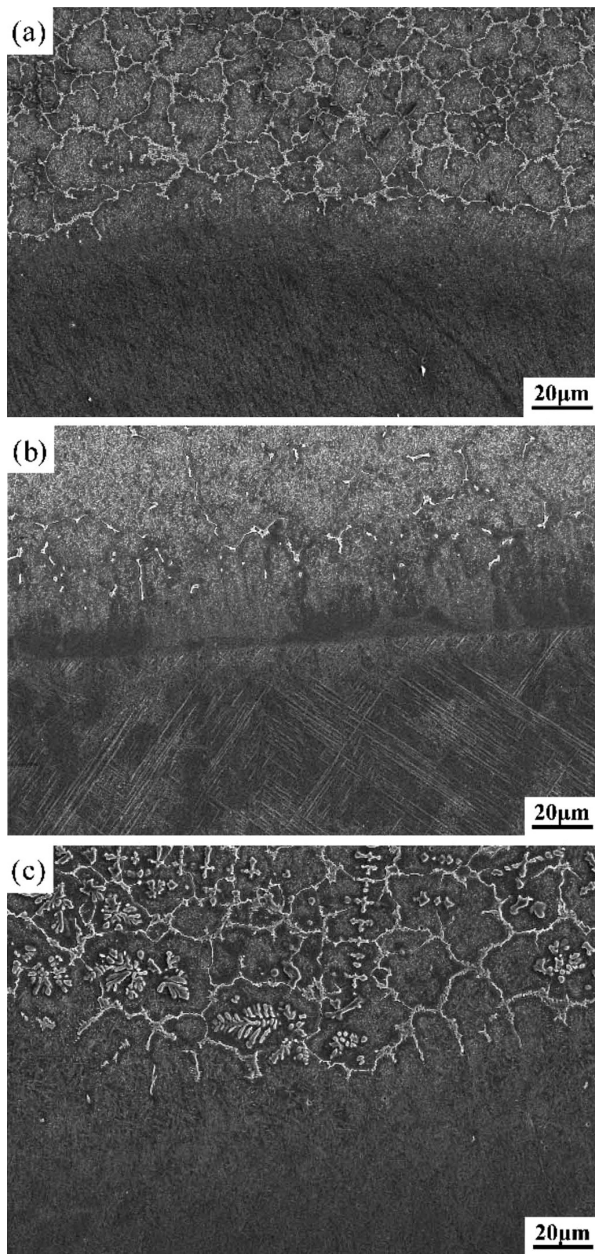


Figure 3: Micrographs of the interfaces in the coatings with different contents of Mo: a) FeCrCoNiAlMo_{0.5}, b) FeCrCoNiAlMo_{1.0}, c) FeCrCoNiAlMo_{1.5}

All the coatings exhibit typical melting-solidifying characteristic, being free of cracks and porosities at the interfaces. A fusion line can be clearly observed at the interface between the substrate and the coatings, which further indicates that a good metallurgical bonding was formed.

Figure 4 shows X-ray diffraction patterns of the coatings. A comparison between the experimental data and the standard values from JCPDS cards (Joint Committee on Powder Diffraction Standards) show that the coatings are mainly composed of the BCC solid solution (no. 03-065-9394) accompanied with the traces of TiC (no. 00-031-1400). When *x* is increased from 0.5 to 1.0, the

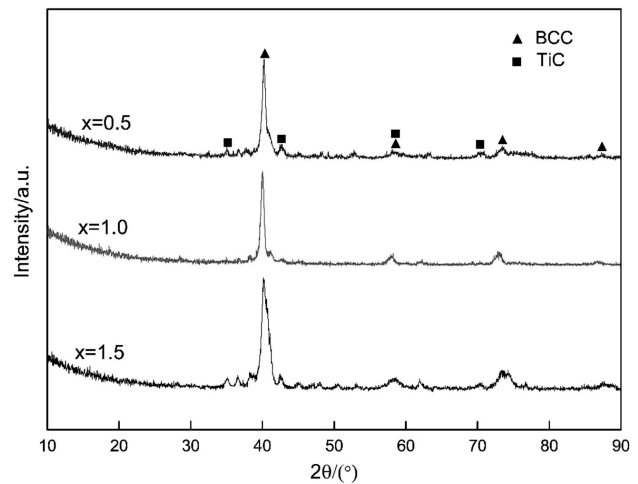


Figure 4: X-ray diffraction patterns of the coatings with different contents of Mo

diffraction peaks related to TiC are significantly decreased in intensity ($2\theta = 35.9^\circ$ and 41.7°) and they even disappear ($2\theta = 72.2^\circ$). However, with *x* increased to 1.5, the diffraction peaks associated with TiC appear again and they even increase in intensity. It can be concluded that a laser-clad HEA coating composed of a single solid solution is successfully synthesized when *x* is 1.0.

Figure 5 shows the cross-sectional microstructures of the coatings with different contents of Mo (*x* = 0.5, 1.0, 1.5). It is obvious that the coatings are mainly composed of three phases with different morphologies, corresponding to fine, gray, rod-like particles (marked as 1), coarse, gray, equiaxed grains (marked as 2) and fine black dendrites (marked as 3). The gray equiaxed phase with the highest fraction volumes can be regarded as the matrix of the coatings, and the other two phases can be seen as the reinforcements. The dendrites are uniformly distributed throughout the whole matrix; however, the rod-like particles are mainly located along the grain boundaries of the matrix. EDS was applied to analyze the chemical compositions of the phases with different morphologies in the coatings. As shown in **Table 1**, the dendritic phase is rich in Ti and C (53.11 at% Ti and 43.84 at% C). Combined with the XRD results, the phase can be confirmed as TiC. The chemical compositions of the two gray phases are rich in Ti, accompanied by Al, Mo, Cr, Co, Fe and Ni with approximately the same atomic content of about 7 at%. It is clear that their chemical compositions are nearly identical, indicating that they belong to the same phase (the BCC solid solution).

The SEM results agree well with the XRD results. For the same phase, the difference in the morphology is closely related to the distribution of metal elements with high molten points during solidification. According to the basic theory of material science, the elements with high molten points concentrate in the pre-crystallized region and are scarce in the post-crystallized region.

Among the elements used in this study, the molten point of Mo (Mo at 2617 °C) is much higher than those of the other elements (Cr at 1857 °C, Fe at 1535 °C, Co at 1495 °C, Ni at 1453 °C, Al at 660 °C), its content in the pre-crystallized equiaxial phase (8.84 at%) is higher

than that in the post-crystallized rod-like phase (7.05 at%). It is clear that the content of black dendrites is decreased when x increases from 0.5 to 1.0, showing an increasing tendency with x being further increased to 1.5. The microstructural-observation results coincide well with the XRD results.

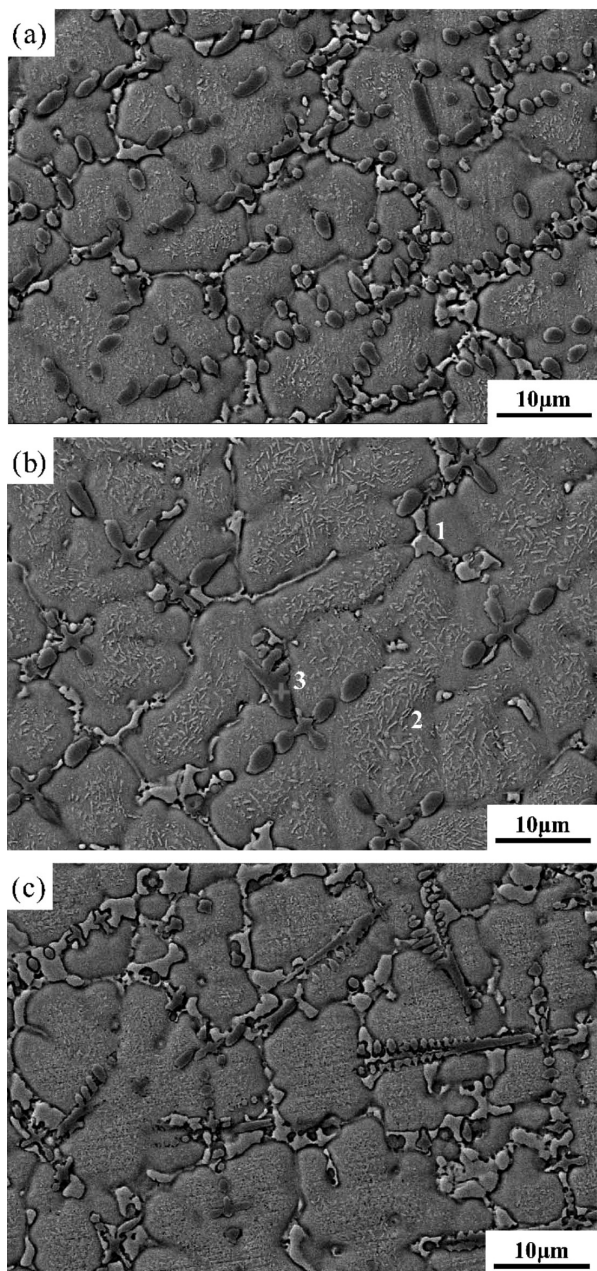


Figure 5: Microstructures of the coatings with different contents of Mo: a) $x = 0.5$, b) $x = 1.0$, c) $x = 1.5$

Table 1: Chemical compositions of the marked zones from the coating shown in Figure 5

Areas	Compositions (at%)							
	Al	Mo	Ti	C	Cr	Fe	Co	Ni
1	9.53	7.05	51.57	0.32	7.27	7.79	8.07	8.40
2	6.83	8.84	51.69	0.29	8.52	8.08	7.94	7.81
3	0.80	0.42	53.11	43.84	0.26	0.35	0.46	0.77

Figure 6 shows the microhardness profiles throughout the cross-sections of the coatings. According to the change in the microhardness, the sample can be divided into three zones, namely, the coating, the transition area and the substrate. The average hardness of the three coatings is 759.4 HV_{0.2} ($x = 0.5$), 857.2 HV_{0.2} ($x = 1.0$) and 844.3 HV_{0.2} ($x = 1.5$). The hardness of the coatings is superior to that of the substrate (330 HV_{0.2}), which should be attributed to the solution- and dispersion-strengthening effects. The hardness of coating ($x = 1.5$) is considerably close to that of coating ($x = 1.0$), which is higher than that of coating ($x = 0.5$). This phenomenon is mainly associated with the difference in the content of alloying elements in the coatings with the change in the content of Mo. The dilution rate is similar (about 62.24 %) for two coatings ($x = 0.5$ and 1.0). Therefore, a larger addition of Mo ($x = 1.0$) means that the higher content of Mo in the coating can improve the solution-strengthening effect. As a result, a higher hardness can be obtained in coating ($x = 1.0$) when compared with that of coating ($x = 0.5$). When x is further increased to 1.5 in the cladding material, the coating should contain a higher content of Mo. However, as it is accompanied with a significant increase in the dilution rate from about 62.24 % to 72.68 %, the content of Mo in coating ($x = 1.5$) is even slightly lower than that in coating ($x = 1.0$). Consequently, the hardness of coating ($x = 1.5$) is similar to that of coating ($x = 1.0$).

Besides, it should be noted that the hardness of the coatings prepared in this study is not inferior to the products synthesized with other surface-engineering techniques such as the process of nitriding. W. H. Wang et al.²⁶ synthesized a porous titanium nitrided coating

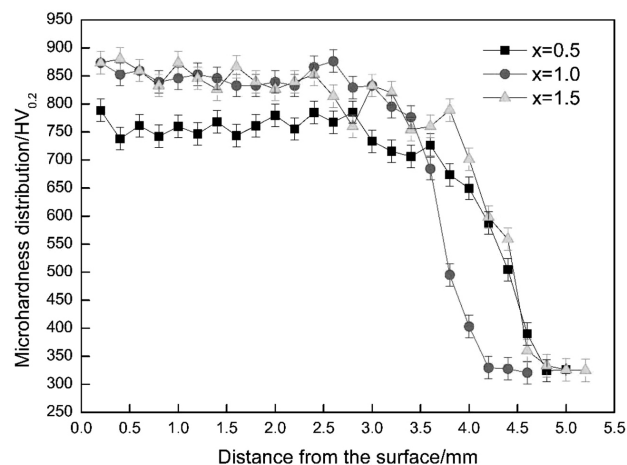


Figure 6: Microhardness profiles along the cross-sections of the coatings

with a thickness of 20 μm on a Ti surface, and the hardness of the coating was 618.68 HV. In the research of C. Yang et al.³, the hardness of the nitrided coating prepared on a new type of metastable β titanium alloy (TB8) was about 850-900 HV. However, the hardness of the coating was extremely unstable and rapidly fell to 700 HV when the distance from the surface was 70 μm . For a nitrided coating, a high hardness can be maintained throughout the whole coating (about 2.7 mm in thickness).

Figure 7 shows the changes in the friction coefficients of the substrate and coatings with different contents of Mo. The friction coefficient of the substrate fluctuates more violently, which indicates that the friction environment between the friction pairs is extremely unstable. Its average value (1.04) is also significantly higher than those of the three coatings (0.80 for $x = 0.5$, 0.61 for $x = 1.0$ and 0.78 for $x = 1.5$). The optimal antifriction effect can be obtained for coating ($x = 1.0$) where the friction coefficient is reduced by 41 % compared with that of the substrate. D. S. She et al.²⁷ applied a series of plasma-nitriding processes to improve the tribological properties of titanium. At the optimized nitriding conditions (850 $^{\circ}\text{C}$ for 8 h), a hard nitrided coating with a thickness of about 80 μm exhibited the lowest friction coefficient of about 0.54, which was reduced by 35 % compared with that of the untreated samples (about 0.73). M. Lepicka et al.²⁸ deposited TiN coatings on the Ti6Al4V alloy using the cathodic arc evaporation/physical vapor deposition (CAE-PVD) method. The friction coefficient of the coatings (0.46) was reduced by 8 % compared with that of the substrate (0.50). It can be seen that the friction coefficient of the laser-clad coating (0.61 for $x = 1.0$) is slightly lower than those of the above coatings prepared with the other methods.

Figure 8 shows the wear profiles of the coatings and the substrate. The wear volumes of the coatings with different Mo contents ($x = 0.5, 1.0, 1.5$) are 1.145 ± 0.021

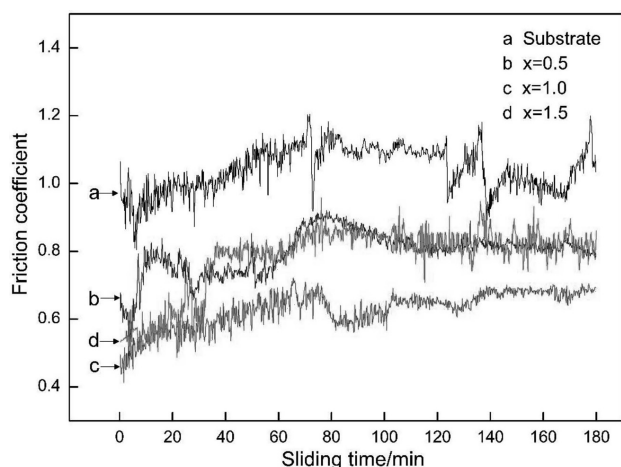


Figure 7: Changes in the friction coefficients of the substrate and coatings

(a deviation of 0.014), 0.823 ± 0.012 (a deviation of 0.011) and $1.219 \pm 0.018 \text{ mm}^3$ (a deviation of 0.015), which are decreased by 51, 65 and 48 %, respectively, when compared with that of the substrate ($2.329 \pm 0.025 \text{ mm}^3$ with a deviation of 0.014). It is also confirmed that the coating with $x = 1.0$ exhibits the optimum wear resistance among the three coatings. Moreover, the wear rates for the substrate and coatings ($x = 0.5, 1.0, 1.5$) can be calculated as follows: 7.19×10^{-5} , 3.53×10^{-5} , 2.54×10^{-5} , $3.76 \times 10^{-5} \text{ mm}^3 \text{ N}^{-1} \text{ m}^{-1}$, respectively. The change in the wear rate of the samples mainly depends on their friction coefficients. When the same load is applied to the samples, a high friction coefficient indicates that a high friction force is generated between the friction pairs, producing a serious micro-cutting effect on the samples' surfaces. More debris is peeled off from the samples, causing an increase in the wear rate. Among all the samples, the wear rate of coating ($x = 1.0$) is the smallest due to its lowest friction coefficient. When compared with coating ($x = 1.0$), the friction coefficients of coatings ($x = 0.5$ and 1.5) are approximately same and higher, resulting in higher wear rates. For the substrate with the highest friction coefficient, the highest wear rate is obtained.

Figure 9 shows the wear morphology of the coatings and the substrate. The wear surface of the substrate is very rough and a large amount of debris can be clearly observed. This indicates that the substrate suffers from very serious micro-cutting during sliding. Comparatively speaking, the wear surfaces of the three coatings are smooth and some fine debris is sporadically distributed, indicating that the wear resistance of the coatings is significantly improved when compared with that of the substrate. Our observation reveals that the wear morphologies of the coatings present a regular change with the increasing Mo content in the cladding materials. On the coating with $x = 0.5$, some fine grooves can be observed, accompanied with some spalling pits and debris. With the increase in the Mo content ($x = 1.0$), only slight scratch traces can be observed and the amount of debris is also significantly reduced. When the content of Mo is

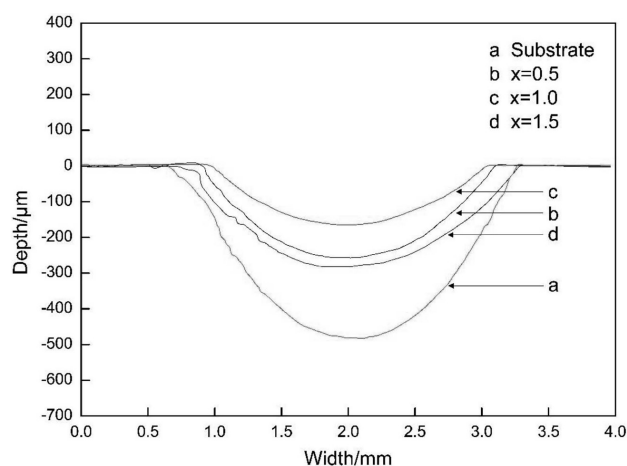


Figure 8: Wear profiles of the substrate and coatings

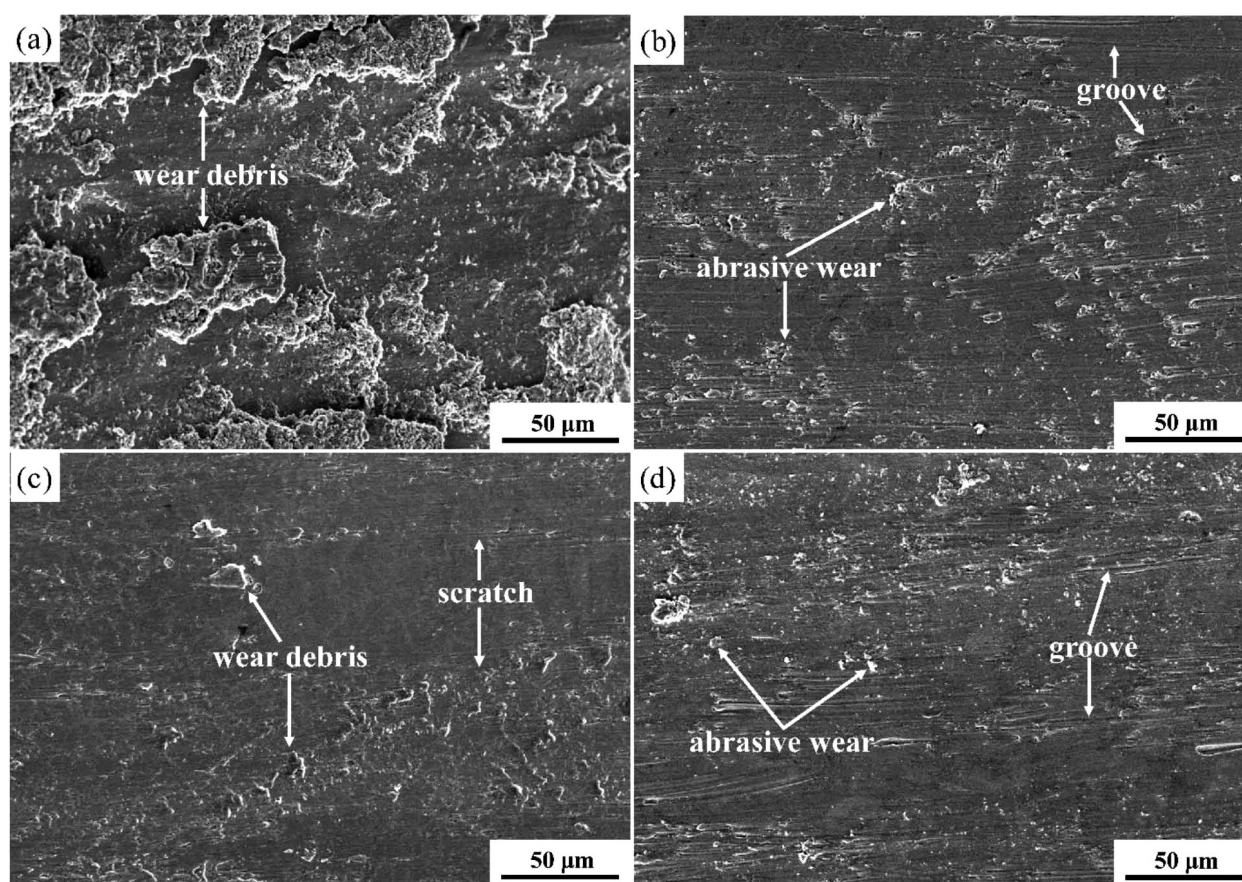


Figure 9: Wear morphology of the coatings and substrates: a) substrate, b) $x = 0.5$, c) $x = 1.0$, d) $x = 1.5$

further increased to $x = 1.5$, the wear morphology of the coating is very similar to that of coating ($x = 0.5$) as again grooves appear on it. The SEM observation clearly indicates that the optimum wear resistance of the coating is obtained when $x = 1.0$, which is completely in accordance with the results of the friction coefficient and wear volume.

4 CONCLUSIONS

In this study, high-entropy-alloy protective coatings of FeCrCoNiAlMox ($x = 0.5, 1.0, 1.5$) were successfully prepared on Ti6Al4V using the laser-cladding process. The coatings were mainly composed of the BCC-solid-solution phase accompanied with traces of TiC. A single solid solution (BCC) was successfully synthesized when $x = 1.0$. Benefited from the effects of solution strengthening and dispersion strengthening, the coatings exhibited excellent mechanical properties. The hardness values for the coatings were 759.4 HV_{0.2}, 857.2 HV_{0.2} and 844.3 HV_{0.2}, respectively, with the increase in x (0.5, 1.0, 1.5). The wear volumes were 1.145 mm³, 0.823 mm³ and 1.219 mm³ and the friction coefficients were 0.80, 0.61 and 0.78. The properties of the coatings were superior to those of the substrate (330 HV_{0.2}, 2.329 mm³, 1.04). The

optimum wear resistance of the coating was obtained when $x = 1.0$.

Acknowledgment

This work was financially supported by the National Natural Science Foundation of China (51471105), Shu Guang project of the Shanghai Municipal Education Commission and the Shanghai Education Development Foundation (12SG44).

5 REFERENCES

- X. J. Jiang, G. Y. Chen, X. L. Men, X. L. Dong, R. H. Han, X. Y. Zhang, R. P. Liu, Ultrafine duplex microstructure and excellent mechanical properties of TC4 alloy via a novel thermo-mechanical treatment, *J. Alloys Compd.*, 767 (2018), 617–621, doi:10.1016/j.jallcom.2018.07.141
- F. Weng, H. J. Yua, J. L. Liu, C. Z. Chen, J. J. Dai, Z. H. Zhao, Microstructure and wear property of the Ti5Si3/TiC reinforced Co-based coatings fabricated by laser cladding on Ti6Al4V, *Opt. Laser Technol.*, 92 (2017), 156–162, doi:10.1016/j.optlastec.2017.01.014
- C. Yang, J. Liu, Intermittent vacuum gas nitriding of TB8 titanium alloy, *Vacuum*, 163 (2019), 52–58, doi:10.1016/j.vacuum.2018.11.059
- S. Takesuea, S. Kikuchic, H. Akebonod, Y. Misakae, J. Komotorif, Effect of pre-treatment with fine particle peening on surface proper-

- ties and wear resistance of gas blow induction heating nitrided titanium alloy, *Surf. Coat. Technol.*, 359 (2019), 476–484, doi:10.1016/j.surfcoat.2018.11.088
- ⁵ C. Lu, J. W. Yao, Y. X. Wang, Y. D. Zhu, J. H. Guo, Y. Wang, H. Y. Fu, Z. B. Chen, M. F. Yan, A novel anti-frictional multiphase layer produced by plasma nitriding of PVD titanium coated ZL205A aluminum alloy, *Appl. Surf. Sci.*, 431 (2018), 32–38, doi:10.1016/j.apsusc.2017.09.082
- ⁶ W. H. Su, Q. Zhao, S. F. Cheng, N. Du, S. X. Wang, Y. Q. Hu, Film structure and frictional wear behaviour of TC4 titanium alloy micro arc oxidation-SiC composite coating, *Surf. Technol.*, 46 (2017), 174–179, doi:10.16490/j.cnki.issn.1001-3660.2017.04.028
- ⁷ V. A. Burdovitsin, D. A. Golosov, E. M. Oks, A. V. Tyunkov, Yu. G. Yushkov, D. B. Zolotukhin, S. M. Zavadsky, Electron beam nitriding of titanium in medium vacuum, *Surf. Coat. Technol.*, 358 (2019), 726–731, doi:10.1016/j.surfcoat.2018.11.081
- ⁸ Q. F. Ye, K. Feng, Z. G. Li, F. G. Lu, R. F. Li, J. Huang, Microstructure and corrosion properties of CrMnFeCoNi high entropy alloy coating, *Appl. Surf. Sci.*, 396 (2017), 1420–1426, doi:10.1016/j.apsusc.2016.11.176
- ⁹ S. Zhang, C. L. Wu, C. H. Zhang, Phase evolution characteristics of FeCoCrAlCuVxNi high entropy alloy coatings by laser high-entropy alloying, *Mater. Lett.*, 141 (2015), 7–9, doi:10.1016/j.matlet.2014.11.017
- ¹⁰ M. Li, J. Gazquez, A. Borisevich, R. Mishra, K. M. Flores, Evaluation of microstructure and mechanical property variations in AlxCoCrFeNi high entropy alloys produced by a high-throughput laser deposition method, *Intermetallics*, 95 (2018), 110–118, doi:10.1016/j.intermet.2018.01.021
- ¹¹ Z. S. Nong, Y. N. Lei, J. C. Zhu, Wear and oxidation resistances of AlCrFeNiTi-based high entropy alloys, *Intermetallics*, 101 (2018), 144–151, doi:10.1016/j.intermet.2018.07.017
- ¹² Y. N. Zhang, S. H. Shu, B. Amit, Additive manufacturing of Ti-Si-N ceramic coatings on titanium, *Appl. Surf. Sci.*, 346 (2015), 428–437, doi:10.1016/j.apsusc.2015.03.184
- ¹³ D. B. Miracle, O. N. Senkov, A critical review of high entropy alloys (HEAs) and related concepts, *Acta Materialia*, 122 (2017), 448–511, doi:10.1016/j.actamat.2016.08.081
- ¹⁴ N. Tüten, D. Canadinc, A. Motallebzadeh, B. Bal, Microstructure and tribological properties of TiTaHfNbZr high entropy alloy coatings deposited on Ti6Al4V substrates, *Intermetallics*, 105 (2019), 99–106, doi:10.1016/j.intermet.2018.11.015
- ¹⁵ H. Li, L. L. MA, C. Q. Wei, L. Sun, W. P. Zhang, Microstructure and properties of laser cladding AlBxCoCrNiTi high-entropy alloy coating on titanium alloys, *Surf. Technol.*, 46 (2017), 226–231
- ¹⁶ Y. F. Juan, J. Li, Y. Q. Jiang, W. L. Jia, Z. J. Lu, Modified criterions for phase prediction in the multi-component laser-clad coatings and investigations into microstructural evolution/wear resistance of FeCrCoNiAlMox laser-clad coatings, *Appl. Surf. Sci.*, 465 (2019), 700–714, doi:10.1016/j.apsusc.2018.08.264
- ¹⁷ Y. Z. Shi, L. Collins, N. Balke, P. K. Liaw, B. Yang, In-situ electrochemical-AFM study of localized corrosion of AlxCoCrFeNi high-entropy alloys in chloride solution, *Appl. Surf. Sci.*, 439 (2018), 533–544, doi:10.1016/j.apsusc.2018.01.047
- ¹⁸ S. Zhang, C. L. Wu, C. H. Zhang, M. Cuan, J. Z. Tan, Laser surface alloying of FeCoCrAlNi high-entropy alloy on 304 stainless steel to enhance corrosion and cavitation erosion resistance, *Opt. Laser Technol.*, 84 (2016), 23–31, doi:10.1016/j.optlastec.2016.04.011
- ¹⁹ G. H. Meng, T. M. Yue, X. Lin, H. O. Yang, H. Xie, D. Xu, Laser surface forming of AlCoCrCuFeNi particle reinforced AZ91D matrix composites, *Opt. Laser Technol.*, 70 (2015), 119–127, doi:10.1016/j.optlastec.2015.02.001
- ²⁰ V. Soare, M. Burada, I. Constantin, D. Mitrica, V. Badilita, A. Caragea, M. Târcolea, Electrochemical deposition and microstructural characterization of AlCrFeMnNi and AlCrCuFeMnNi high entropy alloy thin films, *Appl. Surf. Sci.*, 358 (2015), 533–539, doi:10.1016/j.apsusc.2015.07.142
- ²¹ D. Y. Lin, N. N. Zhang, B. He, G. W. Zhang, Y. Zhang, D. Y. Li, Tribological properties of FeCoCrNiAlBx high-entropy alloys coating prepared by laser cladding, *J. Iron Steel Res. Int.*, 24 (2017), 184–189, doi:10.1016/s1006-706x(17)30026-2
- ²² C. Zhang, B. Huang, P. Q. Dai, Effect of annealing on microstructure and properties of high-entropy FeCoCrNiB/SiC alloy coating prepared by laser cladding, *Met. Heat Treat.*, 41 (2016), 82–88
- ²³ Y. M. Tan, J. S. Li, Z. W. Tang, J. Wang, H. C. Kou, Design of high-entropy alloys with a single solid-solution phase: Average properties vs. their variances, *J. Alloys Compd.*, 742 (2018), 430–41, doi:10.1016/j.jallcom.2018.01.252
- ²⁴ Y. H. Lv, J. Li, Y. F. Tao, L. F. Hu, High-temperature wear and oxidation behaviors of TiNi/Ti2Ni matrix composite coatings with TaC addition prepared on Ti6Al4V by laser cladding, *Appl. Surf. Sci.*, 402 (2017), 478–494, doi:10.1016/j.apsusc.2017.01.118
- ²⁵ H. P. Jin, J. G. Chen, Calculation of the critical parameters for the elastic contact of rigid sphere and plane, *J. Mech. Tran.*, 37 (2013), 49–51
- ²⁶ W. H. Wang, B. J. Xue, L. T. Guo, Y. Fan, B. Li, Y. H. Ling, Y. H. Qiang, Laser nitriding and fusion of bonding porcelain coating on Ti surface, *J. Alloys Compd.*, 777 (2019), 392–396, doi:10.1016/j.jallcom.2018.10.391
- ²⁷ D. S. She, W. Yue, Z. Q. Fu, C. B. Wang, X. K. Yang, J. J. Liu, Effects of nitriding temperature on microstructures and vacuum tribological properties of plasma-nitrided titanium, *Surf. Coat. Technol.*, 264 (2015), 32–40, doi:10.1016/j.surfcoat.2015.01.029
- ²⁸ M. Łępicka, M. Grądzka-Dahlke, D. Pieniak, K. Pasierbiewicz, K. Kryńska, A. Niewczas, Tribological performance of titanium nitride coatings: A comparative study on TiN-coated stainless steel and titanium alloy, *Wear*, 423 (2019), 68–80, doi:10.1016/j.wear.2019.01.029